

CD20 expression regulates CD37 levels in B-cell lymphoma – implications for immunotherapies

Malgorzata Bobrowicz^{a*}, Aleksandra Kusowska^{a,b,c*}, Marta Krawczyk^{a,c,d}, Andriy Zhylyko^{a,b,c}, Christopher Forcados^e, Aleksander Slusarczyk^{a,f}, Joanna Barankiewicz^{g,h}, Joanna Domagala^a, Matylda Kubacz^a, Michal Šmídaⁱ, Lenka Dostalova^j, Katsiaryna Marhelava^a, Klaudyna Fidyta^a, Monika Pepek^a, Iwona Baranowska^{a,c}, Anna Szumera-Cieckiewicz^{k,l}, Else Marit Inderberg^m, Sébastien Wälchli^e, Monika Granica^{a,b,c}, Agnieszka Graczyk-Jarzynka^c, Martyna Majchrzak^m, Marcin Poreba^{j,m,n}, Carina Lynn Gehlert^o, Matthias Peipp^{j,o}, Malgorzata Firczuk^c, Monika Prochorec-Sobieszek^o, and Magdalena Winiarska^{a,c}

^aDepartment of Immunology, Medical University of Warsaw, Warsaw, Poland; ^bDoctoral School, Medical University of Warsaw, Warsaw, Poland; ^cLaboratory of Immunology, Mossakowski Medical Research Institute, Polish Academy of Sciences, Warsaw, Poland; ^dDoctoral School of Translational Medicine, Mossakowski Medical Research Institute, Polish Academy of Sciences, Warsaw, Poland; ^eTranslational Research Unit, Department of Cellular Therapy, Department of Oncology, Oslo University Hospital, Oslo, Norway; ^fDepartment of General, Oncological and Functional Urology, Medical University of Warsaw, Warsaw, Poland; ^gDepartment of Hematology, Institute of Hematology and Transfusion Medicine, Warsaw, Poland; ^hFaculty of Medicine, Lazarski University, Warsaw, Poland; ⁱCentral European Institute of Technology (CEITEC), Masaryk University, Brno, Czech Republic; ^jDepartment of Biology, Faculty of Medicine, Masaryk University, Brno, Czech Republic; ^kDepartment of Pathology, Maria Skłodowska-Curie National Research Institute of Oncology, Warsaw, Poland; ^lBiobank, Maria Skłodowska-Curie National Research Institute of Oncology, Warsaw, Poland; ^mFaculty of Chemistry, Wrocław University of Science and Technology, Wrocław, Poland; ⁿFaculty of Medicine, Wrocław University of Science and Technology, Wrocław, Poland; ^oDivision of Antibody-Based Immunotherapy, Department of Medicine II, Kiel University and University Medical Center Schleswig-Holstein, Kiel, Germany

ABSTRACT

Rituximab (RTX) plus chemotherapy (R-CHOP) applied as a first-line therapy for lymphoma leads to a relapse in approximately 40% of the patients. Therefore, novel approaches to treat aggressive lymphomas are being intensively investigated. Several RTX-resistant (RR) cell lines have been established as surrogate models to study resistance to R-CHOP. Our study reveals that RR cells are characterized by a major downregulation of CD37, a molecule currently explored as a target for immunotherapy. Using CD20 knockout (KO) cell lines, we demonstrate that CD20 and CD37 form a complex, and hypothesize that the presence of CD20 stabilizes CD37 in the cell membrane. Consequently, we observe a diminished cytotoxicity of anti-CD37 monoclonal antibody (mAb) in complement-dependent cytotoxicity in both RR and CD20 KO cells that can be partially restored upon lysosome inhibition. On the other hand, the internalization rate of anti-CD37 mAb in CD20 KO cells is increased when compared to controls, suggesting unhampered efficacy of antibody drug conjugates (ADCs). Importantly, even a major downregulation in CD37 levels does not hamper the efficacy of CD37-directed chimeric antigen receptor (CAR) T cells. In summary, we present here a novel mechanism of CD37 regulation with further implications for the use of anti-CD37 immunotherapies.

ARTICLE HISTORY

Received 28 August 2023
Revised 9 May 2024
Accepted 28 May 2024

Keywords



B-cell lymphoma;
immunotherapy; rituximab;
CD20; CD37; CAR T-cells

Introduction


Diffuse large B-cell lymphoma (DLBCL) is the most frequent non-Hodgkin lymphoma (NHL) subtype, accounting for about 40% of NHL cases and is also one of the most aggressive subtypes.¹ For years, the first-line therapy in DLBCL has been R-CHOP – a combination of chemotherapeutics with rituximab – an anti-CD20 monoclonal antibody (mAb). Although the treatment is mostly well tolerated and efficient, approximately 40% of the patients face relapse characterized by a very poor prognosis and the median survival following relapse not exceeding 6 months.² In recent years, considerable progress has been made in the registration of novel therapies used as a second-line treatment which shows the effectiveness of

immunotherapeutic approaches like antibodies and antibody drug-conjugates directed against CD19 or CD79b molecules as well as CD19 CAR-T cell formulations. Numerous clinical trials are currently underway exploring new molecular targets against aggressive lymphomas including those testing CD37-directed immunotherapies (e.g. Phase 1 clinical trials of CD37-directed CAR T cells – NCT04136275).

The molecular changes induced by RTX and leading to a failure of the next-line therapies have been widely studied in established B-cell lymphoma cell lines with induced resistance to RTX.^{3–5} These models confirmed CD20 downregulation already reported in R-CHOP – treated patients.^{6–8} In this study, we have sought to thoroughly characterize the RTX-

CONTACT Magdalena Winiarska  mwiniarska@imdik.pan.pl  Laboratory of Immunology, Mossakowski Medical Research Institute, Polish Academy of Sciences, Warsaw 02-106, Poland

*equal contribution.

 Supplemental data for this article can be accessed online at <https://doi.org/10.1080/2162402X.2024.2362454>

© 2024 The Author(s). Published with license by Taylor & Francis Group, LLC.

This is an Open Access article distributed under the terms of the Creative Commons Attribution-NonCommercial License (<http://creativecommons.org/licenses/by-nc/4.0/>), which permits unrestricted non-commercial use, distribution, and reproduction in any medium, provided the original work is properly cited. The terms on which this article has been published allow the posting of the Accepted Manuscript in a repository by the author(s) or with their consent.

resistant cell lines to better understand their phenotype. Our analyses revealed a significant downregulation of CD37 molecule on the surface of RR cells. CD37, a tetraspanin protein with structural similarity to CD20, is expressed at the highest levels in the B-cell lineage from pre-B to mature B cells.^{9,10} Alike CD20, CD37 is absent on the surface of plasma cells, making it a suitable target for immunotherapy. In fact, numerous anti-CD37 targeting immunotherapies are currently under investigation.^{11–14} Besides being a molecular target for immunotherapies, CD37 is an important player in the biology of B-cell malignancies¹⁵ as demonstrated in murine models, where CD37 has been described as a negative regulator of lymphomagenesis.¹⁶ Recently, CD37 has been reported to inhibit the fatty acids (FA) transporter FATP1, so CD37-negative lymphoma cells take advantage of increased FA uptake and process exogenous palmitate into energy supporting their increased proliferation.¹⁷ In line with this observation, CD37 presence on the cell surface has been shown to correlate with overall survival (OS) and progression-free survival (PFS) in DLBCL patients.¹⁸ As patients with high CD37 expression showed improved survival on R-CHOP regardless of CD20 expression,¹⁸ CD37 has been suggested to act as a “molecular facilitator” of rituximab action in a yet undefined mechanism. Intriguingly, surface CD37 levels have been shown to correlate with CD20 levels as assessed by flow cytometry in DLBCL cell lines.¹⁸ In this study, using RR and CD20 KO cell lines, we investigated the role of CD20 in regulating CD37 levels and its consequences for the efficacy of various immunotherapeutic approaches targeting CD37.

Materials and methods

Cell culture

All the cell lines were cultured at 37°C in a fully humidified atmosphere of 5% CO₂ in RPMI-1640 (Invitrogen), supplemented with 10% heat-inactivated fetal bovine serum (FBS), 100 U/mL of penicillin, and 100 µg/mL of streptomycin. Cells were passaged every other day. Rituximab-resistant cell lines and their wild-type counterparts were kindly provided by Prof F. Hernandez-Ilizaliturri from Roswell Park, NY, US (human non-Hodgkin's diffuse large B-cell lymphoma: RL, U2932 cell lines) or generated at the Central European Institute of Technology, Czech Republic (human Burkitt lymphoma Ramos cell lines) or in Department of Immunology, Medical University of Warsaw (human Burkitt lymphoma Raji and human diffuse large B-cell lymphoma DHL-4 cell lines). Human non-Hodgkin's diffuse large B-cell lymphoma OCI-Ly-7 (named Ly7 in this paper) and HEK-293T cell lines used for lentivirus production were purchased from DSMZ. Daudi cells (31) were purchased from ATCC.

Retroviral T cells transduction

Peripheral blood mononuclear cells (PBMCs) were isolated from buffy coats from healthy donors by density gradient centrifugation using Lymphoprep™ (STEMCELL Technologies Canada, Inc.). This procedure was approved by the Bioethics Committee of the Medical University of Warsaw,

Poland. Following isolation, PBMCs were seeded onto 6-well plate at density 2×10^6 cells/mL in full RPMI-1640 medium and stimulated for 48 h with anti-CD3 (1:1000) and anti-CD28 (1:1000) mAbs (Invitrogen). After 48 h, stimulated PBMCs were collected and seeded onto a 24-well plate coated with 50 µg/ml retronectin (TakaraBio) at a density of 1×10^6 cells/mL. For retroviral transduction, two rounds of spinoculation with non-concentrated retroviral supernatants were performed (1 h, 1250 rpm, 32°C). Six hours following the second spinoculation, viral supernatants were replaced with full RPMI-1640 medium supplemented with 200 U/ml IL-2 (PeproTech) and Dynabeads Human T-Activator CD3/CD28 at ratio 1:0.3 (Thermo Fisher Scientific).

Constructs

The CAR construct used in this study is the same as the one previously tested in.¹² Briefly, the scFv of the HH1 anti-CD37 antibody was designed with the orientation VL-VH and linked with a (G4S)₄ linker. HH1 scFv was linked to the coding sequence of the CD8 hinge/TM and a second-generation signaling tail (4-1BB-CD3z). This CD37CAR coding sequence was subcloned using Gateway technology (Invitrogen) into the retroviral plasmid pMP71, as depicted in.¹⁹ The coding sequence is the following: METDTLLLVVLLLVVPGSTGDIVMTQSHKLLSTSVGDRVSIITCKASQDVSTAVDWYQQKPGQSPKLLINWASTRHTGVPDRFTGSGSGTDYTLTISSMQAEDLALYYCRQHYSTPFTFGSGTKLEIKGGGGSGGGSGGGSGGGSGGGGSEIQLQSGPELVKPGASVKVSKASGYSFTDYNMYWVKQSHGKSLEWIGYIDPYNGDITTYNQKFKGKATLTVDKSSSTAFIHLNLSLTSSESAVYYCARSPYGHYAMDYWGQGTSTVTVSSDPFVVPVFLPAKPTTTPAPRPPTPAPTIASQPLSLRPEACRPAAGGAVHTRGLDFACDIYIWAPLAGTCGVLLLSLVITLYCNHRNRFVSVVKKRGRKLLLYIFKQPFMRPVQTTQEEDGCSCRFPEEEEGGCELRVKFSRSADAPAYQQGQNQLYNELNLGRREEYDVLDRRGRDP-EMGGKPRRKNPQEGLYNELQKDKMAEAYSEIGMKGERRR-GKGHDGLYQGLSTATKDTYDALHMQALPPR.

The plasmid encoding the GFP-firefly luciferase (GFP-Luc) fusion protein coding sequence was subcloned from an original plasmid obtained from Dr Rainer Löw.

PLA assay

Duolink® Proximity Ligation Assay kit (Sigma Aldrich) was used to determine the interaction between CD20 and CD37. Briefly, Raji and U2932 NTC and CD20 KO cells were incubated with anti-CD37 mouse Ab (M-B371 clone, BD) and anti-CD20 human Ab (obinutuzumab, Roche). Relevant negative controls were performed using isotype antibodies. Cells incubated with anti-CD20 human and anti-CD20 mouse antibodies served as a positive control. Afterward, the cells were incubated with anti-human and anti-mouse probes followed by in situ ligation and amplification according to the manufacturer's protocol. Duolink® Green Detection kit was used to detect protein interactions, and the cells were analyzed on BD Fortessa.

Generation of naratuximab MMAE conjugate

Naratuximab MMAE conjugate was generated by the conjugation of anti-CD37 mAb (naratuximab from Selleckchem) with monomethyl auristatin E (MMAE) using 2 different

dipeptide linkers: VC (valine-citrulline) and VdC (valine-D-citrulline) synthesized as described in.²⁰ The payload was conjugated with 50 µg of anti-CD37 antibody (Natuximab) using the protocol outlined at <https://web.stanford.edu/group/nolan/protocols.html>. Firstly, the disulfide bonds in the antibody were reduced using TCEP according to a standard protocol (TCEP:antibody ratio 10:1, 30 minutes, 37°C). Subsequently, the reduced antibody was incubated with Mal-(PEG)²-Val-Cit-PABC-MMAE at neutral pH for 1 h. Unreacted payload was removed by filtration, and the concentration of the obtained ADCs was measured by absorbance. Additionally, the ADC was subjected to SDS-PAGE analysis under reduced and non-reduced conditions. The resulting ADCs were compared with unconjugated anti-CD37 to demonstrate the shift in molecular weight. The other ADCs were synthesized in a similar manner.

Immunohistochemistry of primary DLBCL samples

Two tissue microarrays were prepared from archival formalin-fixed, paraffin-embedded (FFPE) blocks from DLBCL patients diagnosed at the Institute of Hematology and Transfusion Medicine, Warsaw. From each case, two 1 mm cores were evaluated. The slides were stained with anti-CD37 (clone 2B8; Thermo Fisher Scientific, pH 6.0, 1:200), anti-CD20 and anti-CD19 mAbs (Dako, RTU). The positive controls included lymphoid tissue in the tonsil, appendix, and spleen. CD37 surface expression was scored as negative (<5%) and positive (≥5%) as previously reported,¹⁸ CD20 and CD19 surface were positive according to criteria of WHO Classification of Tumours of Haematopoietic and Lymphoid Tissues 2017.

Patients' sample analysis

We retrospectively analyzed 47 patients diagnosed with DLBCL at the Institute of Hematology and Transfusion Medicine, Warsaw, Poland. Following patients' diagnosis subsequent data were obtained: age, sex, disease stage according to Ann Arbor classification, treatment response determined by Lugano criteria,²¹ progression-free, and overall survival (PFS and OS, respectively). All patients received R-CHOP regimen as first-line treatment. The data collection was conducted according to the Declaration of Helsinki, and the protocol was approved by the Ethics Committee of the Institute of Hematology and Transfusion Medicine, Warsaw, Poland.

In vivo tumor models

Experiments were performed on female NSG (NOD scid gamma) mice bred in-house and maintained in pathogen-free conditions under an approved institutional animal care protocol. Animals were injected via tail vein on day 0 with 5×10^5 Raji WT or RR cells modified with the pMP71-Luc-T-GFP plasmid. Mice were injected intraperitoneally with D-Luciferin potassium salt to confirm engraftment using in vivo imaging system (IVIS spectrum, PerkinElmer). The luciferase signal was used to randomize the animals into groups with equal tumor load. Mice were treated with 10×10^6 CD37-CAR T cells injected intravenously on days 1 and 4. Tumor growth was monitored by IVIS analysis. The study

design was approved by the Ethics Committee of the Medical University of Warsaw (WAW2/042/2024).

Statistical analysis

Results were plotted with GraphPad Prism. Statistical significance was assessed by appropriate tests provided in figure legends. The *p*-values were marked with asterisks on the charts (**p* < 0.05, ***p* < 0.01, ****p* < 0.001, *****p* < 0.0001).

Results

Decrease in CD20 is a hallmark of RR cells

RR cells provide an *in vitro* model for investigating the consequences of prolonged exposure of tumor cells to rituximab.^{4,22} As already reported by others,^{4,22} CD20 downregulation is a hallmark of RR cells (Figure 1A, Suppl. Figure 1A), which largely contributes to their resistance to RTX in complement-dependent cytotoxicity (CDC) (Figure 1B). Moreover, these cells are resistant to RTX *in vivo* as assessed by mice survival (Suppl. Figure 1B) and tumor burden (Suppl. Figure 1C). To investigate the biological consequences of CD20 decrease, we generated models of CD20 KO in several B-cell lymphoma cell lines using CRISPR-Cas9 technology (Figure 1C, Suppl. Figure 1D). All generated CD20 KO cells were characterized with resistance to rituximab (Figure 1D).

CD20 KO cells are characterized with diminished CD37 levels

In order to investigate the consequences of CD20 downregulation, we characterized the surfaceome of CD20 KO cell lines by multi-color flow cytometry using the panel of mAbs against B-cell specific surface-restricted proteins (Figure 2A). Although we observed changes in the levels of several antigens, the only universal change for all the generated CD20 KO cell lines, except CD20 downregulation, was a decrease in the expression of CD37 (Figure 2A,B Suppl. Figure 2A). We further confirmed CD37 decrease in 5 consecutive CD20 KO cell lines in whole-cell lysates using Western blotting (Figure 2C, Suppl. Figure 2B). Interestingly, we found no significant decrease in CD37 mRNA in CD20-deficient cells (Figure 2D). Given the body of research showing synergistic action of anti-CD20 and anti-CD37 mAbs and suggesting close proximity of these two proteins,^{23,24} we sought to investigate if they form a complex in the cell membrane. Indeed, using Duolink Proximity Ligation flow cytometry-based assay which enables the detection of proteins within 40 nm distance (Figure 2E), we observed the amplification generating green fluorescent signal in the presence of both anti-CD37 and anti-CD20 antibodies (Figure 2F, Suppl. Figure 2C). These results clearly demonstrated that CD20 and CD37 are close partners within the cell membrane. To understand their mutual regulation, we generated CD37 KO in Ramos cell line using the CRISPR-Cas9 approach, sorted out a pool, and selected clones of CD37-negative cells (Suppl. Figure 2D,E). We did not observe any reduction in CD20 levels associated with CD37 KO (Figure 2G). These findings suggest that CD20 and CD37

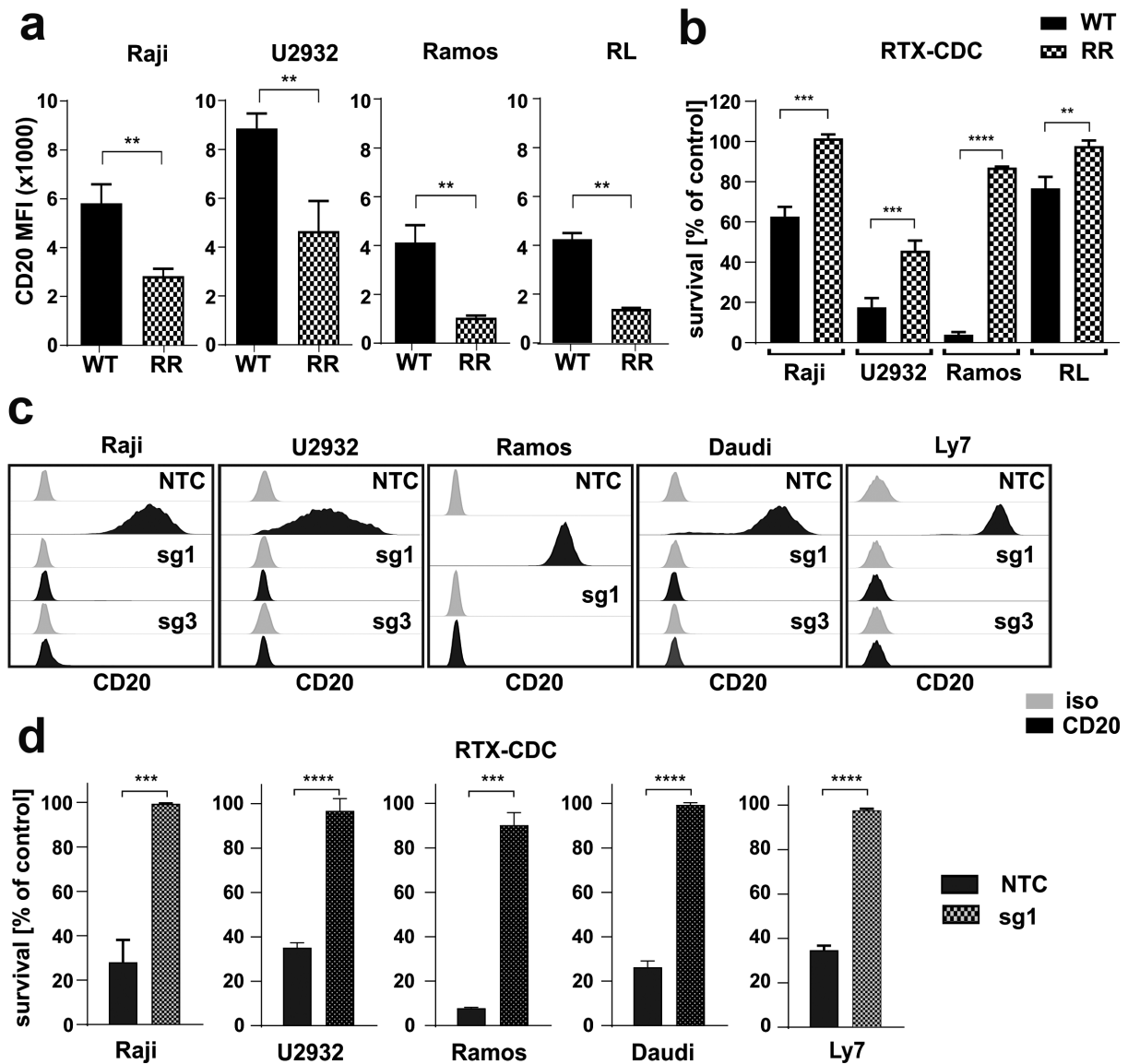


Figure 1. Decrease in CD20 is a hallmark of RTX-resistant cells. (a) RTX-resistant (RR) cells were stained with FITC-conjugated anti-CD20 mAb. Dead cells were discriminated upon staining with PI. The results are presented as mean fluorescence intensity (MFI) of WT and RR cells (mean \pm SD). Statistical significance was determined with Welch's *t*-test, $**p < 0.01$ vs controls. (b) Equal amounts of WT and RR cells were incubated for 1 h (Raji, Ramos) or 4 h (U2932, RL) with 100 μ g/mL (Raji, U2932, RL) or 10 μ g/mL (Ramos) rituximab and 20% human AB serum as a source of complement. Cell viability was assessed with PI staining. The survival of cells is presented as a percentage of control cells without antibody (mean \pm SD). Statistical significance was determined using unpaired *t*-test, $**p < 0.01$, $***p < 0.001$, $****p < 0.0001$ vs control WT cells. (c) Raji, U2932, Ramos, Daudi and Ly7 cells were stably transduced with sgRNA (sg1 or sg3) silencing CD20 or with non-targeting control RNA (sgNTC). The levels of CD20 were assessed with flow cytometry. Representative overlays of CD20 MFI are presented. (d) Equal amounts of NTC and CD20 KO cells (sg1) were incubated for 1 h (Raji, Ramos, Ly7, Daudi) or 4 h (U2932) with 100 μ g/mL (Raji, U2932, Ly7, Daudi) or 10 μ g/mL (Ramos) rituximab and 20% human AB serum as a source of complement. Cell viability was assessed with PI staining. The survival of cells is presented as a percentage of control cells without antibody (mean \pm SD). Statistical analysis was performed using unpaired *t*-test, $**p < 0.01$, $***p < 0.001$, $****p < 0.0001$ vs controls. The experiments were repeated independently four times.

are closely associated on the cell membrane and that CD20 regulates the CD37 protein levels in a posttranscriptional mechanism.

CD37 is downregulated in RR cells

Next, we assessed the levels of CD37 in RR lymphoma cell lines characterized by CD20 downregulation (Figure 1A). In fact, CD37 was significantly down-regulated in all RR cell lines both on the cell surface (Figure 3A, Suppl. Figure 3A) as well as in total cell lysates (Figure 3B, Suppl. Figure 3B). Furthermore, in RR cells we have observed altered expression of several other antigens (Suppl. Figure 3C) which reflects a multifaceted effect

of RTX on B-cell phenotype and existence of several mechanisms underlying the observed changes. Interestingly, the CD37 negative phenotype of RR cells persisted *in vivo* in mice inoculated with RR Ramos cells as demonstrated by the staining on the cells isolated from the spleen (Suppl. Figure 3D). Moreover, in primary samples obtained from DLBCL patients before the start of first-line treatment, expression of CD37 was heterogeneous with approximately 50% of the cases expressing CD37 in less than 5% of the cells, as assessed by immunohistochemistry (Figure 3C). Our results confirm the findings reported by Xu-Monette et al.,¹⁸ showing that CD37-negative status significantly predicted unfavorable PFS following R-CHOP therapy (Figure 3D). Our clinicopathological observations were

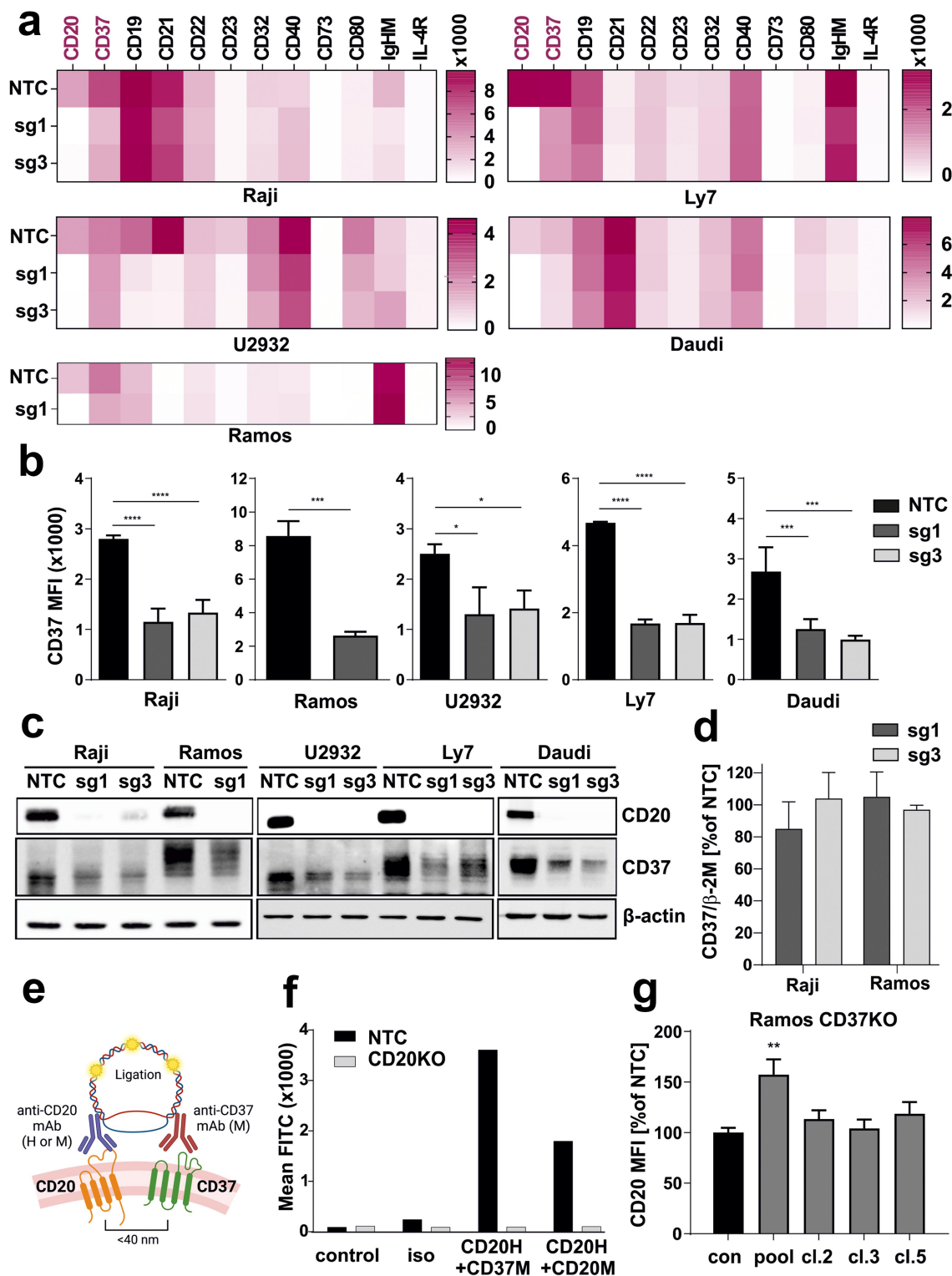


Figure 2. CD20 KO cells are characterized with diminished CD37 levels. (a) NTC and CD20 KO cells were stained with specific fluorochrome-conjugated antibodies targeting surface proteins typical for B-cells. The results are presented as heatmaps. (b) NTC and CD20 KO cells were stained with FITC-conjugated anti-CD37 mAb. Dead cells were discriminated upon staining with PI. The results are presented as MFI of NTC and CD20 KO cells (mean \pm SD). Statistical significance was determined using 1-way ANOVA (NTC vs. sg1 or sg3) or with Welch's *t*-test (NTC vs sg1) * $p < 0.05$, *** $p < 0.001$, **** $p < 0.0001$ vs controls. (c) The levels of CD20 and CD37 were assessed with Western blotting in whole-cell lysates from NTC and CD20 KO cells. β -actin was used as a loading control. (d) cDNA from Raji and Ramos NTC and CD20 KO – sg1 and sg3 cells were used for qRT-PCR amplification of CD37 and β -2 M. Relative reverse transcription quantitative polymerase chain reaction expression of CD37 gene was calculated by the user non-influent second derivative method and shown as log-transformed target to reference ratio. β -2 M gene served as a reference. (e) Proximity ligation experiment design. Cells of interest were incubated with saturating amounts of unlabeled human anti-CD20 mAb and mouse anti-CD37 mAb. Following incubation with anti-human and anti-mouse probes, in situ ligation and amplification, the formed protein complexes were analyzed in flow cytometry. (f) PLA assay was performed in Raji NTC and sg1 cell lines to prove the formation of complex between CD20–CD37. The results are presented as MFI from a representative experiment. The experiments were repeated independently three times. (g) Ramos WT cells were edited with CD37-targeting sgRNA, CD37-negative cells were sorted on a FACS sorter, and single-cell clones were generated. Non-targeting sgRNA (NTC) was used as a negative control. CD20 expression was assessed by flow cytometry. The results are presented as a percentage of MFI of control NTC cells (mean \pm SD). Statistical analysis was performed using 1-way ANOVA, ** $p < 0.01$.

limited to the newly diagnosed DLBCL cases ($n = 47$) treated with R-CHOP in a first-line setting. Based on these experiments, we conclude that low/decreased CD37 expression can be relatively frequent in patients. Since CD37 is explored as a therapeutic target, in the subsequent steps, we investigated the consequences of decreased CD37 levels on the efficacy of various forms of therapy targeting CD37.

CD37 decrease leads to impaired efficacy of CD37 mAbs-mediated CDC, which can be restored using lysosome inhibitors

A decrease in the target antigen directly translates into impaired efficacy of mAbs that exert cytotoxicity in complement-dependent mechanism.^{25,26} Therefore, we asked if decreased CD37 in RR and CD20 KO cells influence the efficacy of CDC-inducing anti-CD37 mAb. We observed impaired efficacy of anti-CD37 mAb in CD20 KO and RR cells (Figure 4A and B, respectively). This effect was clearly visible despite utilizing an anti-CD37 mAb with the E430G mutation, which promotes more efficient IgG hexamer formation through intermolecular Fc–Fc interactions after cell surface antigen binding.^{27,28} While in CD20 KO cells a decreased efficacy of anti-CD37 mAb may be solely attributed to decreased CD37 expression, in RR cells it may be the result of both decreased CD37 expression and an increase in complement inhibitor protein CD59 (Suppl. Figure 3E).

Since CD20 and CD37 are interrelated in the plasma membrane, we hypothesized that the mechanism of their interaction is dependent on the internalization, trafficking, and degradation processes. More specifically, we assumed that CD37 endocytosis is accelerated in the cells lacking CD20 and that the presence of CD20 stabilizes CD37 within the cell membrane. To test this assumption, we preincubated Raji NTC and CD20 KO cells with nontoxic concentrations of compounds blocking lysosome-dependent degradation such as chloroquine and bafilomycin A. These inhibitors used up-regulated CD37 levels in both NTC as well as in CD20 KO cells, where they significantly increased CD37 levels nearly to the values observed in NTC cells (Figure 4C, Suppl. Figure 4 A). Increase in CD20 and CD37 levels can also be observed in whole-cell lysates of these cells (Figure 4D, Suppl. Figure 4 B). Accordingly, inhibition of lysosomal degradation increased the efficacy of anti-CD37 mAbs against Raji CD20 KO cells in CDC cytotoxicity assay (Figure 4E). All in all, our results show that CD37 can be degraded by lysosome and the blockage of lysosome can be used as an approach to increase the sensitivity of tumor cells with CD20 KO to anti-CD37 mAbs.

CD20 KO cells show an increased internalization rate of anti-CD37 mAb and enhanced efficacy of ADC targeting CD37

In the further steps, we investigated the potential of the use of anti-CD37 ADCs in the cells with decreased CD20 levels. This treatment approach involves the use of surface antigen-

targeted mAbs to deliver cytotoxic payloads into tumor cells upon conjugate internalization through endocytosis. In our initial experiments, we investigated the internalization rate of anti-CD37 mAb (clone M-B371, mouse anti-human) in NTC and CD20 KO cells and observed its increased internalization. In this experiment, Raji NTC and CD20 KO cells were incubated with equal amounts of mouse anti-human anti-CD37 mAb conjugated with pH-sensitive dye, which becomes activated in lysosomes. For 23 h, the images were registered in IncuCyte every 20 min (Suppl. Figure 4C). Fluorescence AUC was normalized to the cell area (Suppl. Figure 4D). As CD20 KO cells were characterized with decreased CD37 levels, Quantibrite measurement was performed (Suppl. Figure 4E) and the AUC normalized to the number of CD37 molecules per cell (Figure 4F). These results suggest an increased internalization in CD20 KO cells as one of the potential mechanisms involved in the downregulation of CD37 that could be exploited therapeutically with anti-CD37 ADCs. To test this hypothesis, we conjugated naratuximab (K7153A mAb clone) with antimetabolic agent monomethyl auristatin E (MMAE) using valine-citrulline (VC) and valine-D-citrulline (VdC) linkers. Indeed, the internalization rate of naratuximab normalized to the number of CD37 molecules per cell, was markedly increased in Raji RR cells (Figure 4G), leading to improved cytotoxicity of both tested ADCs following 48 h incubation (Figure 4H, Suppl. Figure 4F).

CD37 decrease does not hamper CAR-T cells' cytotoxicity

Since CD37 has recently been designated as a suitable target for CAR-T therapy,^{11,12} we then asked the question if a substantial decrease in its levels would hamper the efficacy of HH1-based anti-CD37 CAR as well. First, we confirmed the decrease in CD37 levels with HH1 antibody (Suppl. Figure 5A). Then, we performed CD37 CAR-T cytotoxicity assays *in vitro* against both RR and CD20 KO cell lines as targets using two effector-to-target (E:T) ratios. We observed that despite significantly diminished CD37 levels in six different cell lines (either RR or CD20 KO cells), the cytotoxicity of the tested CAR T cells was not affected (Figure 5A,B). We further observed that in the human xenograft model, CD37 CAR-T cells impaired tumor growth as monitored by bioluminescence (Suppl. Figure 5B) and prolonged mice survival (Figure 5C) in groups inoculated with either Raji WT or Raji RR cell line. We concluded that CD37, although diminished upon downregulation of CD20, was still sufficiently expressed to be detected by CD37 CAR T cells, suggesting that CD37 remains an attractive target for cell-based therapies and could be further explored even in RTX-pretreated patients.

Discussion

Novel treatment modalities for r/r DLBCL patients are intensively pursued. However, little is known about the mechanisms of primary resistance and molecular changes induced by the treatment of the phenotype of lymphoma cells despite the clear unfavorable prognosis of patients progressing during or shortly after first-line immunochemotherapy.²⁹ In the recent few years, the

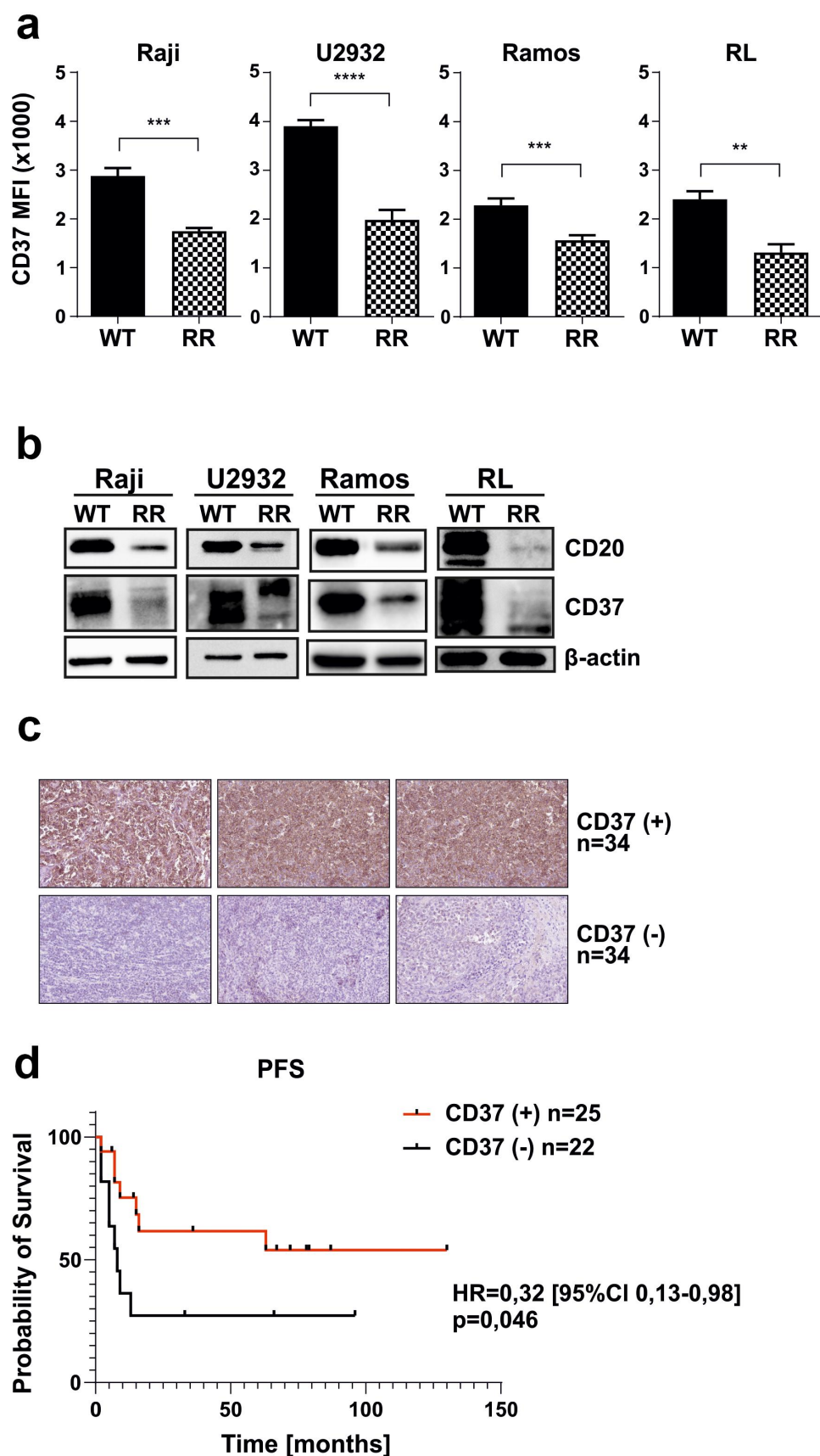


Figure 3. CD37 is downregulated in RR cells. (a) WT and RR cells were stained with FITC-conjugated anti-CD37 mAb. Dead cells were discriminated upon staining with PI. The results are presented as MFI of WT and RR cells (mean \pm SD). Statistical significance was determined with Welch's *t*-test, ** p <0.01, *** p <0.001, **** p <0.0001. The experiments were repeated independently four times. (b) The levels of CD20 and CD37 were assessed with Western blotting in whole-cell lysates. β -actin was used as loading control. The experiments were repeated independently three times. (c) CD37 expression was evaluated in 68 primary paraffin-embedded samples by a pathologist blinded to the clinical data of the patients. Representative stainings for CD37-positive and CD37-negative stainings are shown. (d) Kaplan–Meier curves were plotted for PFS in CD37- and CD37+ patients. The survival curves were compared with Peto and Peto's generalized Wilcoxon test.

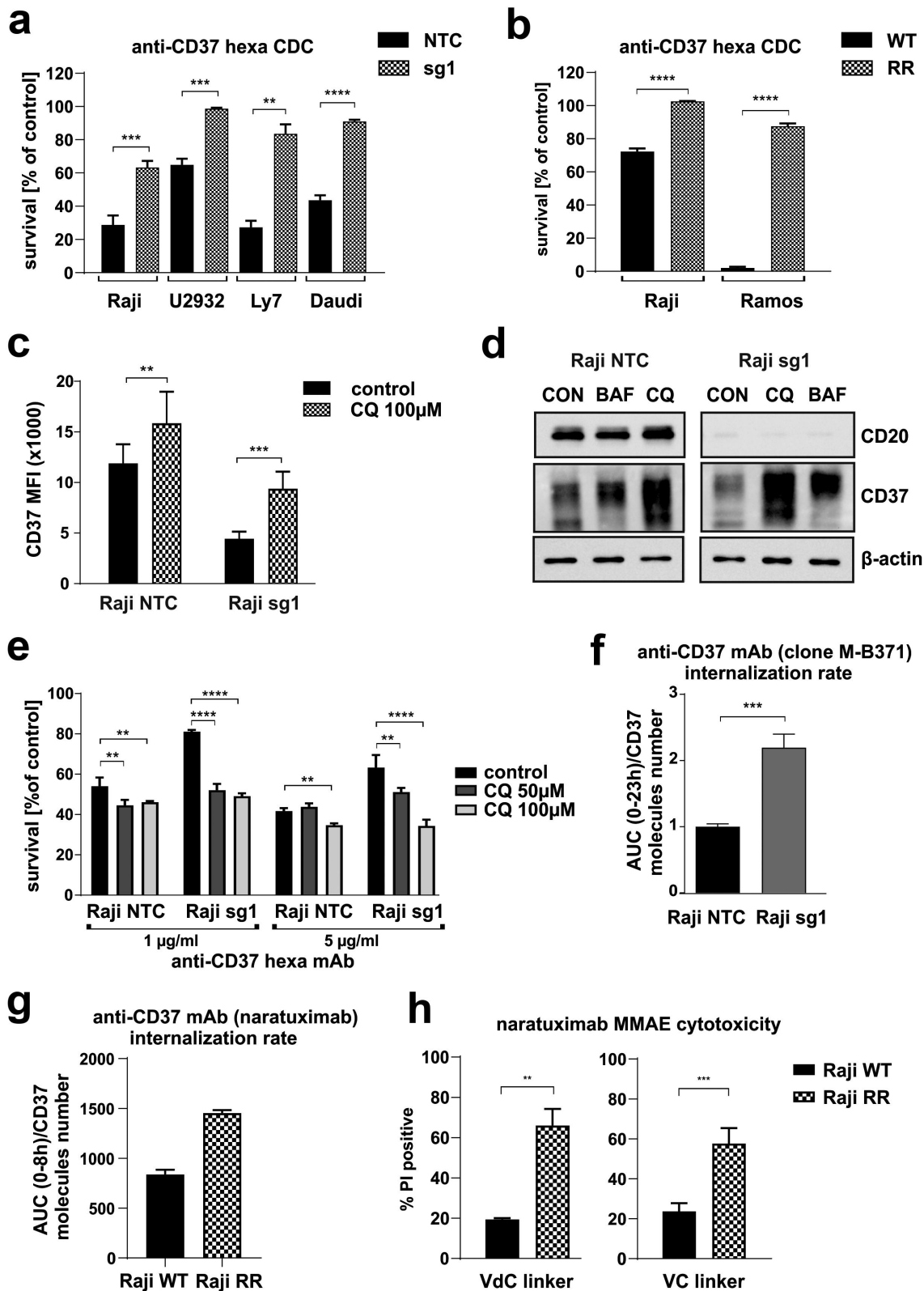


Figure 4. CD37 decrease leads to impaired efficacy of anti-CD37 mAbs-mediated CDC, which can be restored using lysosome inhibitors. Equal amounts of NTC and CD20 KO cells (a) and WT and RR Raji cells (b) were incubated for 1 h (Raji, Ramos, Daudi, Ly7) or 4 h (U2932) with 10 μ g/ml anti-CD37 mAb and 20% human AB serum as a source of complement. Cell viability was assessed with PI staining. The survival of cells is presented as a percentage of control cells without antibody (mean \pm SD). Statistical significance was determined using unpaired *t*-test, ****p* < 0.001, *****p* < 0.0001 vs controls. (c) Equal amounts of NTC and CD20 KO cells were incubated for 24 h with 100 μ M chloroquine. Thereafter, the cells were stained with PE-conjugated anti-CD37 mAb. The results are presented as MFI of NTC and sg1 cells (mean \pm SD). Statistical significance was determined using 2-way ANOVA with Sidak's post hoc test, ***p* < 0.01, ****p* < 0.001 vs controls (d) The levels of CD20 and CD37 were assessed with Western blotting in whole-cell lysates. β -actin was used as loading control. (e) Equal amounts of NTC and CD20 KO Raji cells preincubated for 24 h with 50 or 100 μ M chloroquine were treated for 1 h with anti-CD37 mAb (5–10 μ g/ml) and 20% human AB serum as a source of complement. Cell viability was assessed with PI staining. The survival of cells is presented as a percentage of control cells without antibody (mean \pm SD). Statistical significance was determined using 2-way ANOVA with Sidak's post hoc test, ***p* < 0.01, *****p* < 0.0001 vs controls. (f) Internalization rate of anti-CD37 mAb (clone M-B371) was determined in Raji NTC and sg1 cells

therapeutic armamentarium for aggressive lymphomas has expanded thanks to registrations of second-line treatments that finally offer an alternative to auto-HSCT, namely anti-CD19 CAR T cells, novel mAbs-based regimens: tafasitamab plus lenalidomide, novel ADCs e.g. polatuzumab vedotin and loncastuximab tesirine as well as bispecific mAbs (epcortimab, glofitamab).³⁰

CD37, a tetraspanin predominantly expressed in B cells, is currently being explored as a target for mAbs, ADCs, and CAR T cells. The results of our work show that strategies targeting CD37 need to be carefully implemented in r/r B-cell lymphoma patients. Using CD20 KO cells, we identified the association between CD37 and CD20. We hypothesize that the expression of the latter plays a crucial role in preventing CD37 from undergoing endocytosis, as suggested by our results in CD20 KO cells where lysosome inhibition increased CD37 levels to the levels seen in control (NTC) cells. This discovery has several implications. First of all, we demonstrate that decreased CD37 expression correlates with reduced efficacy of anti-CD37 mAbs in a complement-dependent mechanism, where the expression of the target antigen determines the cytotoxic effect. However, this limitation may be encompassed by the use of bi-specific antibodies, e.g. targeting CD20 and CD37 that show superior efficacy to anti-CD37 mAbs alone²³ or bi-paratopic mAbs.^{26,31} On the other hand, using ADCs based on the pre-clinically explored ADC – naratuximab emtansine we show that CD20 loss facilitates CD37 endocytosis and it may translate to increased efficacy of anti-CD37 ADCs that have recently been presented as a highly efficient strategy in B-cell malignancies *in vitro* and in murine models.³² The efficacy of ADCs relies on the endocytosis of the target antigen-ADC complex and the release of the cytotoxic payload to the cytoplasm. It has already been reported that rituximab synergizes with naratuximab emtansine by increasing the endocytosis of CD37.²⁴ While it has been recently demonstrated that the efficacy of naratuximab emtansine relies on the expression levels of CD37,³³ our results suggest that anti-CD37 ADCs may be an option also for r/r RTX-treated patients. Interestingly, the recent work by *Arribas et al.*, who explored the resistance mechanism to naratuximab emtansine, demonstrates that acquired resistance to this anti-CD37 ADC may lead to increased sensitivity to venetoclax.³³ This emphasizes the significance of examining the implications of acquired resistance to identify novel therapeutic pathways with a focus on tailored medical approaches. Finally, we show that decreased CD37 levels (up to 50% in our models) do not influence the efficacy of CD37-targeted CARs in both *in vitro* and *in vivo* settings and delineate CD37 CARs as an effective option for CD20-negative RTX-pretreated patients. These findings suggest that despite the decreased expression in RTX-resistant cells, CD37 still hold promise for further investigation.

Decrease in CD37 expression has been reported to affect patients' prognosis negatively, and according to the studies by other groups³⁴ and ours, up to 50% of DLBCL patients show undetectable CD37 protein expression by immunohistochemistry. However, it needs to be emphasized that in the IHC stainings performed by us and others, a clone of anti-CD37 mAb (2B8) used does not correspond to the clone used for CAR construct (HH1 clone). Therefore, in our study, we have not only stained the cells with a diagnostic antibody and assessed CD37 expression by Western blotting but we have also used the HH1 antibody to evaluate changes in the expression of the epitope targeted by CAR T cells. Although we have observed that staining with HH1 clone was also decreased in RR cells, the remaining CD37 antigen was preserved at relatively high levels, sufficient to mediate CD37 CAR T-mediated killing. The discussion on the tumor antigen density required for CAR T cell efficacy has been already raised by others, and it has been shown that antigen density is one of the factors influencing the activity of CAR T cells.^{35,36} While CD28-CD3 ζ -CARs outperform 4-1BB-CD3 ζ -CARs when antigen density is low, in our study CD37-4-1BB-CD3 ζ CAR T cells were already effective in the elimination of RR cells. In our view, these findings suggest that despite its various levels in WT and RR cells CD37 is a suitable target for CAR-T cell therapy, especially considering that CAR-T cells can be reengineered to enhance activity against low-antigen-density tumors.³⁵

Finally, our study sheds new light on the regulation of CD37 expression. So far, CD37 loss has been attributed to decreased expression of a transcriptional factor IRF8.³⁴ However, as demonstrated by the study by Elfrink et al., up to 40% of IRF8 low DLBCL samples still express detectable CD37 in IHC³⁴ suggesting that there are additional factors regulating CD37 expression. Tetraspanins play an important role in the organization of the cellular membrane,³⁷ forming clusters that overlap each other. The CD37 cluster has been shown to overlap with CD81 and CD82 cluster,³⁷ while the latter has been reported to form a supramolecular complex with MHC class I, MHC class II, CD53, and CD20.³⁸ Our results suggest that a decrease in CD20 levels, a protein not belonging to the tetraspanin family but to MS4A family that shows some similar characteristics in the structure, may induce changes in the composition of the cellular membrane and promote degradation of CD37. Other members of MS4A family have already been demonstrated to govern the endocytosis process, i.e. MS4A4A by directing the trafficking of KIT regulates its signaling³⁹ and MS4A3 promotes endocytosis of common β -chain (β c) cytokine receptors.⁴⁰

Overall, our study adds new knowledge to the current state of the art on the regulation of CD37, which in light of recent findings^{11,12,18,26,31,32} constitutes an attractive therapeutic target for immunotherapies. The results of our study once again

incubated in IncuCyte with equal amounts of mAb conjugated to pH sensitive dye activated in lysosome. Statistical significance was determined using unpaired *t*-test, ****p*<0.001 vs controls. (g) Internalization rate of anti-CD37 mAb (clone K7153A) was determined in Raji WT and RR cells incubated in IncuCyte with equal amounts of mAb conjugated to pH sensitive dye activated in lysosome. The internalization rates are shown as fluorescence AUC normalized to number of CD37 molecules per cell. (h) Equal amounts of Raji WT and RR cells were incubated for 48 h with 1 μ g/ml of two anti-CD37 ADC variants with VC (valine-citrulline) or VdC (valine-D-citrulline) linkers. Cell viability was assessed with PI staining. Cytotoxicity of ADCs is presented as a percentage of PI-positive cells (mean \pm SD) vs untreated cells. Statistical analysis was performed using unpaired *t*-test, ***p*<0.01, ****p*<0.001 vs controls.

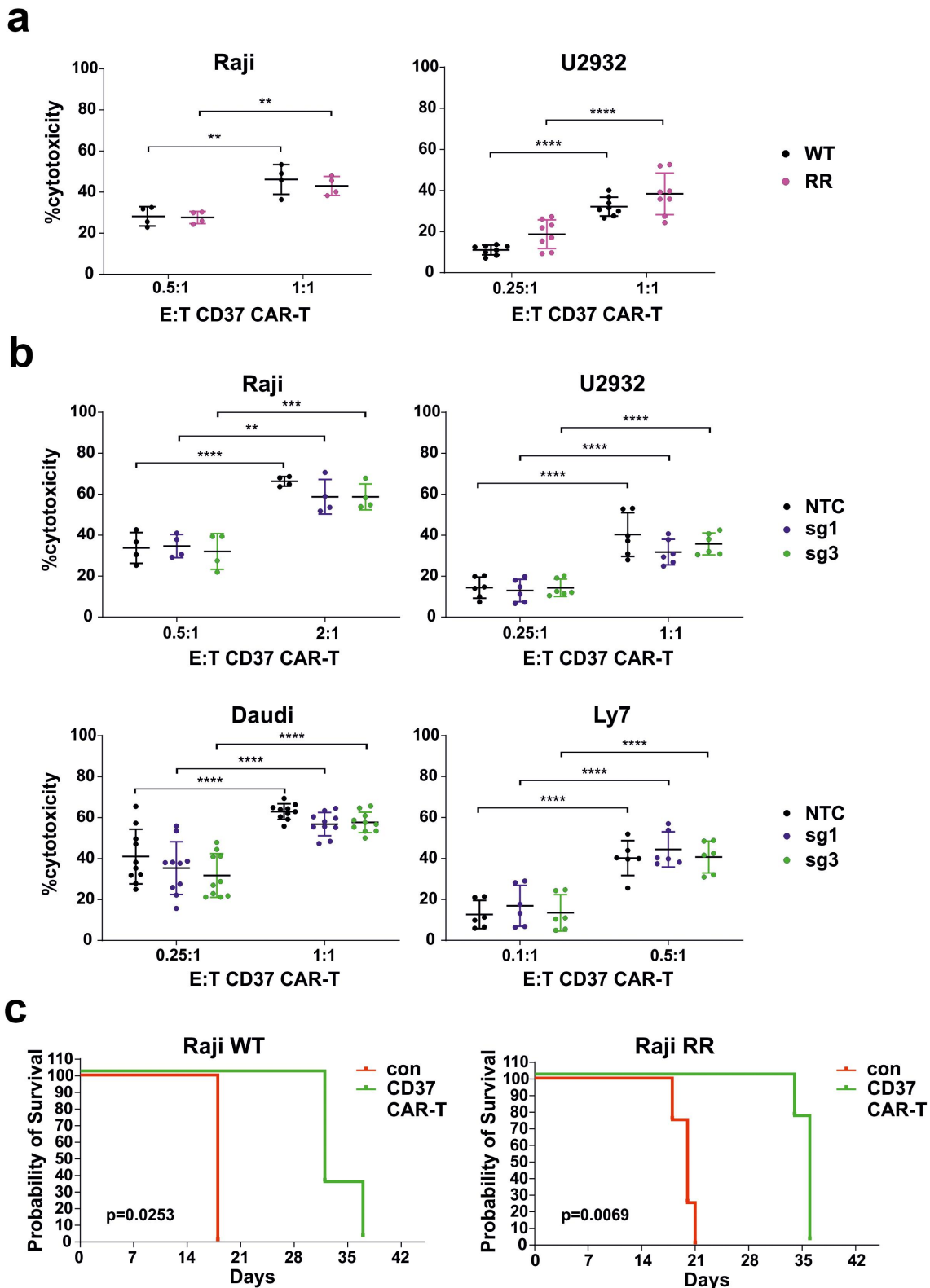


Figure 5. CD37 decrease does not hamper CAR T cells' cytotoxicity. Equal amounts of (a) WT and rituximab-resistant (RR) or (b) NTC and sg1 cells were stained with CellTrace™ Violet and incubated for 16 h with various effector to target (E:T) ratios of CD37 CAR-T cells. Cell viability was assessed with flow cytometry following PI staining. Data represent mean \pm SD of % cytotoxicity of CD37 CAR-T cells after subtracting cytotoxicity of unmodified T-cells. Statistical analysis was performed using 2-way ANOVA with Tukey's post hoc test. Experiments were repeated at least four times (c) Kaplan–Meier survival curve of mice inoculated on day 0 with 5×10^5 Raji WT (left panel, $n = 3$ mice per group) or RR (right panel, $n = 4$ mice per group) after two doses of 10×10^6 CAR-T cells injected intravenously on day 1 and 4. Statistical significance was determined using the long-rank test.

prove that CD37 is highly variable in DLBCL patients. Finally, we show that immunotherapy using anti-CD37 CAR T cells can be an effective option despite low levels of CD37 protein.

Acknowledgments

The authors would like to thank Prof F. Hernandez-Izalurri, Prof M. Czuczman and Cory Mavis from Roswell Park, NY, US for providing RR cell lines and Genmab, Utrecht, the Netherlands, for providing CDC-inducing anti-CD37 mAb.

Disclosure statement

No potential conflict of interest was reported by the author(s).

Funding

This work was supported by Polish National Science Centre 2019/35/D/NZ5/01191 (MB), Polish National Science Centre 2022/45/N/NZ6/01691 (AK), National Centre for Research and Development within POLNOR program NOR/POLNOR/ALTERCAR/0056/2019 (PI: Magdalena Winiarska), a research grant MUNI/A/1558/2023 (MŚ) and by the project National Institute for Cancer Research (Programme EXCELES, ID Project No. LX22NPO5102) - Funded by the European Union - Next Generation EU (MŚ). SW and EMI were partially supported by Barnkreftforeningen (PERCAP), KLINBEFORSK (#AML-CD37/2022) and NFR KSP-2021 CellFit project (326811). MP and MM are supported by the NCN grant (2020/39/I/NZ5/03104).

ORCID

Malgorzata Bobrowicz  <http://orcid.org/0000-0002-9078-5168>
 Christopher Forcados  <http://orcid.org/0009-0003-5073-1522>
 Else Marit Inderberg  <http://orcid.org/0000-0002-6147-3536>
 Sébastien Wälchli  <http://orcid.org/0000-0001-5869-1746>
 Magdalena Winiarska  <http://orcid.org/0000-0001-5605-3329>

Authors' contribution:

M.B. designed the study, performed and analyzed experiments and wrote the manuscript, A.K. performed and analyzed experiments and was involved in manuscript preparation; M.K., A.S., J.D., M.Ku., M.S., L.D., K.M., K.F., C.F., M.P., I.B., M.G., A.G.-J., C.L.G. performed and analyzed experiments, AZ performed in vivo study and analyzed data, J.B. provided primary material and analyzed patients' data, A.S.-C. performed immunohistochemistry analysis, E.M.I. and S.W. provided different constructs, cells and CAR CD37 T cells and were involved in manuscript preparation. M.M. and M. P. synthesized and characterized anti-CD37 ADCs. M.P., M.F. and M.P.-S. provided expert advice and guidance throughout the study, M.W. designed the study, wrote the manuscript, prepared the figures and provided expert guidance throughout the study; all authors reviewed the manuscript.

Data availability statement

Raw data will be made available upon reasonable request from the corresponding author.

References

- Shaw J, Harvey C, Richards C, Kim C. Temporal trends in treatment and survival of older adult diffuse large B-Cell lymphoma patients in the SEER-Medicare linked database. *Leuk Lymphoma* gruzdzień. 2019;60(13):3235–3243. doi:10.1080/10428194.2019.1623886.
- Glass B, Dohm AJ, Truemper LH, Pfreundschuh M, Bleckmann A, Wulf GG, Rosenwald, Ziepert M, Schmitz N, I in A. et al. Refractory or relapsed aggressive B-cell lymphoma failing (R)-CHOP: an analysis of patients treated on the RICOVER-60 trial. *Ann Oncol Off J Eur Soc Med Oncol*. 2017 1 gruzdzień 28 (12):3058–3064. doi:10.1093/annonc/mdx556.
- Jazirehi AR, Vega MI, Bonavida B. Development of Rituximab-Resistant Lymphoma Clones with Altered Cell Signaling and Cross-Resistance to Chemotherapy. *Cancer Res*. 2007 1. 67(3):1270–1281. doi:10.1158/0008-5472.CAN-06-2184.
- Olejniczak SH, Hernandez-Izalurri FJ, Clements JL, Czuczman MS. Acquired resistance to rituximab is associated with chemotherapy resistance resulting from decreased Bax and Bak expression. *Clin Cancer Res*. [2008 Mar 1]. 14(5):1550–1560. doi:10.1158/1078-0432.CCR-07-1255.
- Takei K, Yamazaki T, Sawada U, Ishizuka H, Aizawa S. Analysis of changes in CD20, CD55, and CD59 expression on established rituximab-resistant B-lymphoma cell lines. *Leuk Res*. 2006 1. 30 (5):625–631. doi:10.1016/j.leukres.2005.09.008.
- Kennedy GA, Tey SK, Cobcroft R, Marlton P, Cull G, Grimmett K, Thomson, Gill D, I in D, Gill D. Incidence and nature of CD20-negative relapses following rituximab therapy in aggressive B-cell non-Hodgkin's lymphoma: a retrospective review. *Br J Haematol listopad*. 2002;119(2):412–416. doi:10.1046/j.1365-2141.2002.03843.x.
- Maeshima AM, Taniguchi H, Nomoto J, Maruyama D, Kim SW, Watanabe T, Kobayashi, Tobinai K, Matsuno Y, I in Y. et al. Histological and immunophenotypic changes in 59 cases of B-cell non-Hodgkin's lymphoma after rituximab therapy. *Cancer Sci*. 2009;100(1):54–61. doi:10.1111/j.1349-7006.2008.01005.x.
- AACR Annual Meeting. Itinerary Planner. <https://www.abstractsonline.com/pp8/#!/10517/presentation/21748>.
- de Winde Cm, Zuiderwoude M, Vasaturo A, van der Schaaf A, Figdor CG, van Sriel AB, de Winde CM. Multispectral imaging reveals the tissue distribution of tetraspanins in human lymphoid organs. *Histochem Cell Biol sierpień*. 2015;144(2):133–146. doi:10.1007/s00418-015-1326-2.
- Barrena S, Almeida J, Yunta M, López A, Fernández-Mosteirín N, Giralt M, Romero, Perdiguier L, I in M, Perdiguier L. et al. Aberrant expression of tetraspanin molecules in B-cell chronic lymphoproliferative disorders and its correlation with normal B-cell maturation. *Leukemia sierpień*. 2005;19(8):1376–1383. doi:10.1038/sj.leu.2403822.
- Scarfò I, Ormhøj M, Frigault MJ, Castano AP, Lorrey S, Bouffard AA, van Scoyk A, Rodig SJ, Shay AJ. et al. Anti-CD37 chimeric antigen receptor T cells are active against B- and T-cell lymphomas. *Blood*. 2018 4. 132(14):1495–1506. doi:10.1182/blood-2018-04-842708.
- Köksal H, Dillard P, Josefsson SE, Maggadottir SM, Pollmann S, Fåne A, Blaker, I in YN, Beiske K, Huse K. et al. Preclinical development of CD37CAR T-cell therapy for treatment of B-cell lymphoma. *Blood Adv*. 2019 12. 3(8):1230–1243. doi:10.1182/bloodadvances.2018029678.
- Okuno S, Adachi Y, Terakura S, Julamanee J, Sakai T, Umemura K, Miyao, I in K, Goto T, Murase A. et al. Spacer Length Modification Facilitates Discrimination between Normal and Neoplastic Cells and Provides Clinically Relevant CD37 CAR T Cells. *J Immunol Baltim Md*. 2021 15. 1950; 206(12):2862–2874. doi:10.4049/jimmunol.2000768.
- Golubovskaya V, Zhou H, Li F, Valentine M, Sun J, Berahovich R, Xu, I in S, Quintanilla M, Ma MC. et al. Novel CD37, Humanized CD37 and Bi-Specific Humanized CD37-CD19 CAR-T Cells Specifically Target Lymphoma. *Cancers*. 2021 26. 13(5):981. doi:10.3390/cancers13050981.
- Bobrowicz M, Kubacz M, Slusarczyk A, Winiarska M. CD37 in B Cell Derived Tumors—More than Just a Docking Point for Monoclonal Antibodies. *Int J Mol Sci styczeń*. 2020;21(24):9531. doi:10.3390/ijms21249531.
- de Winde Cm, Veenbergen S, Young KH, Xu-Monette ZY, Zy X-M XX, Xia II, Y CM, Jabbar KJ, van den Brand M, van der Schaaf A. et al. Tetraspanin CD37 protects against the development of B cell

- lymphoma. *J Clin Invest Luty.* 2016;126(2):653–666. doi:10.1172/JCI81041.
17. Peeters R, Cuenca-Escalona J, Zaal EA, Hoekstra AT, Balvert ACG, Vidal-Manrique M, Blomberg, van Deventer SJ, Stienstra R, Jellusova J. et al. Fatty acid metabolism in aggressive B-cell lymphoma is inhibited by tetraspanin CD37. *Nat Commun.* 2022 13. 13(1):5371. doi:10.1038/s41467-022-33138-7.
 18. Xu-Monette ZY, Li L, Byrd JC, Jabbar KJ, Manyam GC, Maria de Winde C, van den Brand, I in M, Tzankov A, Visco C. et al. Assessment of CD37 B-cell antigen and cell of origin significantly improves risk prediction in diffuse large B-cell lymphoma. *Blood.* 2016 29. 128(26):3083–3100. doi:10.1182/blood-2016-05-715094.
 19. Wälchli S, Löset GÅ, Kumari S, Johansen JN, Yang W, Sandlie I, Olweus, I in J, Olweus J. A practical approach to T-cell receptor cloning and expression. *PLoS One.* 2011;6(11):e27930. doi:10.1371/journal.pone.0027930.
 20. Cauculitan NG, Dela Cruz Chuh J, Ma Y, Zhang D, Kozak KR, Liu Y, Pillow, I in TH, Sadowsky J, Cheung TK. et al. Cathepsin B Is Dispensable for Cellular Processing of Cathepsin B-Cleavable Antibody-Drug Conjugates. *Cancer Res.* 2017 15. 77 (24):7027–7037. doi:10.1158/0008-5472.CAN-17-2391.
 21. Cheson BD, Fisher RI, Barrington SF, Cavalli F, Schwartz LH, Zucca E, Lister, Lister TA, I in TA. Recommendations for initial evaluation, staging, and response assessment of Hodgkin and non-Hodgkin lymphoma: the Lugano classification. *J Clin Oncol Off J Am Soc Clin Oncol.* 2014 20. 32(27):3059–3067. doi:10.1200/JCO.2013.54.8800.
 22. Czuczman MS, Olejniczak S, Gowda A, Kotowski A, Binder A, Kaur H, Knight, Starostik P, I in J, Starostik P. et al. Acquirement of Rituximab Resistance in Lymphoma Cell Lines Is Associated with Both Global CD20 Gene and Protein Down-Regulation Regulated at the Pretranscriptional and Posttranscriptional Levels. *Clin Cancer Res.* [2008 Mar 1]. 14(5):1561–1570. doi:10.1158/1078-0432.CCR-07-1254.
 23. Oostindie SC, van der Horst HJ, Lindorfer MA, Cook EM, Tupitza JC, Zent CS, Burack, van der Horst HJ, I in R, VanDermeid KR. et al. CD20 and CD37 antibodies synergize to activate complement by Fc-mediated clustering. *Haematologica wrzesień.* 2019;104(9):1841–1852. doi:10.3324/haematol.2018.207266.
 24. Hicks SW, Lai KC, Gavrilescu LC, Yi Y, Sikka S, Shah P, Kelly, I in ME, Lee J, Lanieri L. et al. The Antitumor Activity of IMG529, a CD37-Targeting Antibody-Drug Conjugate, Is Potentiated by Rituximab in Non-Hodgkin Lymphoma Models. *Neoplasia.* 2017 1. 19(9):661–671. doi:10.1016/j.neo.2017.06.001.
 25. van MT, Rs van R, Hol S, Hagenbeek A, Ebeling SB. Complement-Induced Cell Death by Rituximab Depends on CD20 Expression Level and Acts Complementary to Antibody-Dependent Cellular Cytotoxicity. *Clin Cancer Res.* 2006 1. 12(13):4027–4035. doi:10.1158/1078-0432.CCR-06-0066.
 26. Oostindie SC, van der Horst HJ, Kil LP, Strumane K, Overdijk MB, van den Brink En, van den Brakel, van der Horst HJ, van den Brink EN, I in JHN. et al. DuoHexaBody-CD37[®], a novel biparatopic CD37 antibody with enhanced Fc-mediated hexamerization as a potential therapy for B-cell malignancies. *Blood Cancer J.* 2020 28. 10(3):30. doi:10.1038/s41408-020-0292-7.
 27. de Jong Rn, Beurskens FJ, Verploegen S, Strumane K, van Kampen Md, Voorhorst M, Horstman, de Jong RN, van Kampen MD, I in W. et al. A Novel Platform for the Potentiation of Therapeutic Antibodies Based on Antigen-Dependent Formation of IgG Hexamers at the Cell Surface. *PLoS Biol styczeń.* 2016;14(1):e1002344. doi:10.1371/journal.pbio.1002344.
 28. Strasser J, de Jong Rn, Beurskens FJ, Wang G, Heck AJR, Schuurman J, Parren, Hinterdorfer P, Preiner J, Preiner J. et al. Unraveling the Macromolecular Pathways of IgG Oligomerization and Complement Activation on Antigenic Surfaces. *Nano Lett.* 2019 10. 19(7):4787–4796. doi:10.1021/acs.nanolett.9b02220.
 29. Farooq U, Maurer MJ, Thompson CA, Thanarajasingam G, Inwards DJ, Micallef I, Macon, I in W, Syrbus S, Lin T. et al. Clinical heterogeneity of diffuse large B cell lymphoma following failure of front-line immunochemotherapy. *Br J Haematol.* 2017;179(1):50–60. doi:10.1111/bjh.14813.
 30. Ames A, Lee D. Updates in the Diffuse Large B-Cell Lymphoma Treatment Landscape. *J Adv Pract Oncol kwiecień.* 2022;13 (3):341–344. doi:10.6004/jadpro.2022.13.3.33.
 31. van der Horst HJ, Oostindie SC, Cillessen SAGM, Gelderloos AT, Sagm C, Nijhof IS, Zweegman, Chamuleau MED, Mutis T, Breij ECW. et al. Potent Preclinical Efficacy of DuoHexaBody-CD37 in B-Cell Malignancies. *HemaSphere styczeń.* 2021;5(1):e504. doi:10.1097/HS9.0000000000000504.
 32. Vaisitti T, Vitale N, Micillo M, Brandimarte L, Iannello A, Papotti MG, Di Napoli, Orlik C, I in A, Orlik C. et al. Anti-CD37 alpha-amanitin conjugated antibodies as potential therapeutic weapons for Richter's Syndrome. *Blood.* 2022;blood.2022016211. 1(Supplement 1):791–791. doi:10.1182/blood-2021-150280.
 33. Arribas AJ, Gaudio E, Napoli S, Herbaux CJY, Tarantelli C, Bordone RP, I in. PI3Kδ activation, IL6 over-expression, and CD37 loss cause resistance to the targeting of CD37-positive lymphomas with the antibody-drug conjugate naratuximab emtansine [Internet]. bioRxiv; 2023 [accessed 2024 Apr 20]. <https://www.biorxiv.org/content/10.1101/2023.11.14.566994v1>.
 34. Elfrink S, Ter Beest M, Janssen L, Baltissen MP, Pwtc J, Kenyon AN, Steen, I in RM, de Windt D, Hagemann PM. et al. IRF8 is a transcriptional activator of CD37 expression in diffuse large B-cell lymphoma. *Blood Adv.* 2022 4. 6(7):2254–2266. doi:10.1182/bloodadvances.2021004366.
 35. Majzner RG, Rietberg SP, Sotillo E, Dong R, Vachharajani VT, Labanieh L, Myklebust, I in JH, Kadapakkam M, Weber EW. et al. Tuning the Antigen Density Requirement for CAR T-cell Activity. *Cancer Discov. maj* 2020;10(5):702–723. doi:10.1158/2159-8290.CD-19-0945.
 36. Harris DT, Hager MV, Smith SN, Cai Q, Stone JD, Kruger P, Lever, I in M, Dushek O, Schmitt TM. et al. Comparison of T Cell Activities Mediated by Human TCRs and CARs That Use the Same Recognition Domains. *J Immunol Baltim Md 1950.* 2018 1. 200(3):1088–1100. doi:10.4049/jimmunol.1700236.
 37. Zuidschewoude M, Göttfert F, Dunlock VME, Figdor CG, van den Bogaart G, van SA. The tetraspanin web revisited by super-resolution microscopy. *Sci Rep.* 2015 17. 5(1):12201. doi:10.1038/srep12201.
 38. Szöllösi J, Horejsí V, Bene L, Angelisová P, Damjanovich S. Supramolecular complexes of MHC class I, MHC class II, CD20, and tetraspan molecules (CD53, CD81, and CD82) at the surface of a B cell line JY. *J Immunol Baltim Md 1950.* 1996 1. 157 (7):2939–2946. doi:10.4049/jimmunol.157.7.2939.
 39. Cruse G, Beaven MA, Music SC, Bradding P, Gilfillan AM, Metcalfe DD. The CD20 homologue MS4A4 directs trafficking of KIT toward clathrin-independent endocytosis pathways and thus regulates receptor signaling and recycling. *Mol Biol Cell.* 2015 1. 26 (9):1711–1727. doi:10.1091/mbc.E14-07-1221.
 40. Zhao H, Pomicter AD, Eiring AM, Franzini A, Ahmann J, Hwang JY, Senina, I in A, Helton B, Iyer S. et al. MS4A3 promotes differentiation in chronic myeloid leukemia by enhancing common β-chain cytokine receptor endocytosis. *Blood.* 2022 3. 139 (5):761–778. doi:10.1182/blood.2021011802.